J. Fluid Mech. (2019), *vol.* 881, *pp.* 983–1009.
doi:10.1017/jfm.2019.784

Simultaneous and sequential collisions of three wetted spheres

Robert H. Davis†

Department of Chemical and Biological Engineering, University of Colorado Boulder, Boulder, CO 80303, USA

(Received 4 April 2019; revised 31 July 2019; accepted 20 September 2019; first published online 25 October 2019)

Rectilinear collisions of three wetted spheres are considered under conditions of high capillary numbers, for which viscous lubrication forces dominate over capillary forces. The viscous forces resist the relative motion, as characterized by the Stokes number (a dimensionless ratio of particle inertia and viscous forces). At high Stokes numbers, the particles penetrate the fluid layers between them with sufficient inertia that they collide and rebound. Both simultaneous and sequential collisions are simulated, and various outcomes are demonstrated: full agglomeration of the three spheres at low Stokes numbers, full separation or Newton's cradle at large Stokes numbers and even reverse Newton's cradle at intermediate Stokes numbers when there is a thicker combined fluid layer between the two target spheres than between the striker sphere and the first target sphere. When there is an initial air gap between the two target spheres, even more exotic outcomes are predicted, such as full separation after the initial collisions followed by full agglomeration or reverse Newton's cradle (intermediate Stokes numbers) or Newton's cradle (large Stokes numbers) after the subsequent collisions when the striker sphere catches back up to the target spheres. The approach and findings of this work are expected to provide input and guidance to future work on discrete-element modelling of collisions of many wet particles.

Key words: lubrication theory, particle/fluid flow, granular media

1. Introduction

Applications such as particle agglomeration and coating have created interest in modelling granular flows of wetted particles, when both liquid and solid contact forces are present. The basic concepts of an 'elastohydrodynamic' collision between a particle and a solid surface in the presence of liquid were first described over 30 years ago by Davis, Serayssol & Hinch (1986). More recent research has included both normal and oblique collisions between one particle and a surface, or between two particles, either fully immersed in a liquid or with thin liquid layers on the solid surfaces (e.g. Barnocky & Davis 1988; Lian, Adams & Thornton 1996; Joseph *et al.* 2001; Davis, Rager & Good 2002; Joseph & Hunt 2004; Kantak & Davis 2004; Yang & Hunt 2006; Ma, Liu & Chen 2016; Buck *et al.* 2017, 2018). These works identified the Stokes number (ratio of particle inertia to viscous fluid forces) as a key parameter in determining whether or not particle rebound would occur and, if

† Email address for correspondence: robert.davis@colorado.edu

so, the wet coefficient of restitution. Some of these papers also examined additional effects, such as capillary forces, on the collision and rebound of wetted particles. Furthermore, discrete-element methods (DEM) have been extended in recent years to wet granular flows (e.g. Xu, Orpe & Kudrolli 2007; Anand *et al.* 2009; Radl *et al.* 2010; Liu, Yang & Yu 2013) and cohesive flows (Mikami, Kamiya & Horio 1998; Weber & Hrenya 2006). These methods include capillary forces from the liquid bridges between particles, and sometimes viscous forces.

An important contribution was made by Donahue, Hrenya & Davis (2010*a*), Donahue *et al.* (2010*b*), who studied the simultaneous, normal (head-on) collision of three wetted spheres. Through modelling and experiment, they demonstrated four possible outcomes: (i) fully agglomerated (FA), in which the three spheres stick together, (ii) fully separated (FS), in which the spheres bounce apart subsequent to impact and remain separated, (iii) Newton's cradle (NC), in which the striker particle remains agglomerated with the target (middle) sphere, and the third sphere separates from the agglomerated pair, and (iv) reverse Newton's cradle (RNC), in which the striker particle rebounds and separates while the target sphere agglomerates with the third sphere. The modelling treated the simultaneous three-body collisions as a series of two-body collisions.

In the current work, simultaneous and sequential interactions of three wetted spheres are modelled for head-on collisions, with a particular focus on how the viscous lubrication forces acting between the second and third particle affect the relative motion of the first and second particle, and *vice versa*. The overall outcome of a three-body collision is shown to be sensitive to these interactions, as well as to the thickness of the liquid coatings, the Stokes number, and the initial separation of the second and third spheres. The geometry is similar to that considered by Donahue *et al.* (2010*a*,*b*), but the present study investigates both simultaneous and sequential collisions, treats simultaneous collisions as fully three-body collisions rather than as a series of two-body collisions and provides analytical and semi-analytical results for pairwise sequential collisions. The focus is on viscous fluids (such as oils or polymer solutions) and large capillary numbers, for which viscous forces dominate over capillary forces, although it is noted that both viscous and capillary forces can be important for less viscous fluids (such as water) or in cases of small Stokes numbers when the relative velocities are greatly reduced from the initial value. Qualitative agreement is shown between the current model and experiments of Donahue *et al.* (2010*b*).

2. Problem formulation

The rectilinear motion of three spheres is considered as shown in figure 1. Sphere i ($i = 1$, 2 or 3) has mass m_i (including the liquid film) and radius a_i, and is covered with a thin liquid film of thickness $\delta_i \ll a_i$ and viscosity μ. Sphere 1 is the striker sphere and has initial velocity (directed along the line of centres) of magnitude v_1^0. Spheres 2 and 3 are assumed to be initially motionless. Gravity and any other forces except liquid and solid contact forces are neglected. The 1–2 and 2–3 pairs of spheres and their liquid coatings are initially separated by distances d_{12}^0 and d_{23}^0, respectively. The air in the space external to the solid spheres and their liquid coatings is assumed to have negligible effect on the motion of the spheres. The value of $d_{12}^0 \geqslant 0$ is irrelevant, as the interaction starts when this separation has been traversed and the liquid layers of the 1–2 pair first contact (defined as time $t = 0$). In contrast, the value of d_{23}^0 is important, as it determines the time at which the 2–3 interaction starts and if and how this interaction is coupled with the 1–2 interaction.

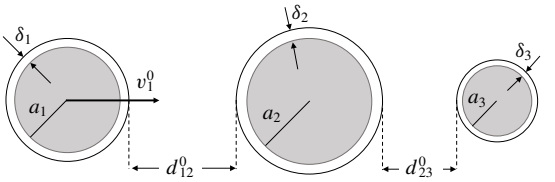

FIGURE 1. Schematic of the initial conditions for the rectilinear collision of three wet spheres.

The motion of each particle is described by Newton's second law,

$$m_1\frac{\mathrm{d}v_1}{\mathrm{d}t} = -F_{12}, \quad m_2\frac{\mathrm{d}v_2}{\mathrm{d}t} = F_{12} - F_{23}, \quad m_3\frac{\mathrm{d}v_3}{\mathrm{d}t} = F_{23}, \tag{2.1a–c}$$

where F_{ij} is the liquid-mediated force acting between the i–j pair of particles. The liquid force is zero prior to contact, which occurs when the distance between the liquid surfaces decreases to $d_{ij} = 0$ and that between the solid surfaces decreases to $h_{ij}^0 = \delta_i + \delta_j$. Once the liquid layers touch, the liquid force may include both a viscous lubrication force, which scales as $O(\mu a_{ij}^2 v_{ij}/h_{ij})$ and a capillary force, which scales as $O(\sigma a_{ij})$, where v_{ij} is the relative velocity of the i and j spheres, a_{ij} is their reduced radius, h_{ij} is the gap thickness between their solid surfaces, and σ is the surface tension. The ratio of viscous and lubrication forces is represented by a modified capillary number, $Ca = 3\mu a v_r/(\sigma h)$, as defined by Donahue *et al.* (2010*a*,*b*), where v_r is the relative velocity of two colliding spheres, a is their reduced radius and h is the minimum separation between their surfaces. Their experiments using viscous oils had $Ca > 3000$, so that capillary forces could be safely neglected, as done in the present simulations. However, capillary forces may be important when low-viscosity fluids are used (see § 6.1). They may also come into play under near-critical conditions for post-collision separation, as the relative velocity and, hence, lubrication forces are small under these conditions as the spheres separate.

Once the liquid layers on two colliding spheres begin to overlap, then the viscous lubrication forces resisting their relative motion are given by (Kantak & Davis 2006),

$$F_{ij} = 0, \quad h_{ij} \geqslant h_{ij}^f; \quad F_{ij} = 6\pi\mu a_{ij}^2 v_{ij}(1 - h_{ij}/h_{ij}^f)^2/h_{ij}, \quad h_{ij} < h_{ij}^f, \tag{2.2a,b}$$

where $a_{ij} = a_i a_j/(a_i + a_j)$ is the reduced radius, $v_{ij} = v_i - v_j$ is the relative velocity of the two spheres along their line of centres and h_{ij}^f is the final film thickness before the two spheres separate during rebound (not including a liquid bridge or filament between the spheres prior to capillary rupture). Normally, $h_{ij}^f = \delta_i + \delta_j$, and the final film thickness is the same as the initial thickness and simply the sum of the individual film thicknesses, as shown in figure 2. However, a larger value of h_{23}^f can occur as a special case, if the 2–3 pair is already in contact at $t = 0$ and there is an excess of liquid in the contact region due to coating the two spheres while they are held together, as described by Donahue *et al.* (2010*a*,*b*).

Since the lubrication force in (2.2) is based on the relative velocity, it is convenient to recast (2.1) in terms of the relative velocity of each pair

$$\frac{\mathrm{d}v_{12}}{\mathrm{d}t} = \frac{-F_{12}}{m_{12}} + \frac{F_{23}}{m_2}, \quad \frac{\mathrm{d}v_{23}}{\mathrm{d}t} = \frac{F_{12}}{m_2} - \frac{F_{23}}{m_{23}}, \tag{2.3a,b}$$

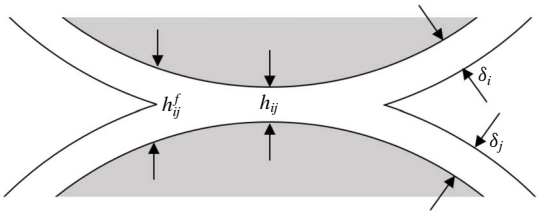

FIGURE 2. Schematic of two wetted spheres in close contact with overlapping liquid layers.

where $m_{ij} = m_i m_j/(m_i + m_j)$ is the reduced mass of the i–j pair. The relative velocities govern the change in gap sizes

$$\frac{\mathrm{d}h_{ij}}{\mathrm{d}t} = -v_{ij}. \tag{2.4}$$

The initial conditions for (2.3) and (2.4) are

$$v_{12} = v_1^0, \quad v_{23} = 0, \quad h_{12} = h_{12}^0 = \delta_1 + \delta_2, \quad h_{23} = h_{23}^0 = d_{23}^0 + \delta_2 + \delta_3 \quad \text{at } t = 0. \tag{2.5a–d}$$

Note that $h_{12}^f = h_{12}^0 = \delta_1 + \delta_2$, so that the 1–2 pair separates once it has rebounded to its initial separation, and any residual effects of a liquid bridge and capillary forces are neglected. The same is true of the 2–3 pair, except in the special case where it is initially agglomerated with excess fluid in the near-contact region.

3. Rebound criteria

Once the collision starts, the 1–2 gap decreases due to a positive relative velocity, v_{12}. The lubrication force F_{12} reduces this relative velocity, and it also pushes sphere 2 towards sphere 3, so that the 2–3 gap also decreases. If the Stokes number (ratio of particle inertia to viscous forces, defined in the next section) is small, then viscous dissipation will eventually bring the relative motion to rest, so that the gaps no longer decrease and the spheres remain agglomerated or stuck together. However, if the Stokes number is large, the particles have sufficient inertia that the gap between a particle pair will continue to decrease until a critical or minimum separation, h_{min}, is reached and rebound is initiated. As described by Donahue *et al.* (2010*b*), there are (at least) three different physical scenarios that would give rise to a minimum gap and subsequent rebound: (i) *solid–solid contact* – although lubrication forces would prevent physical contact (i.e. $h_{ij} \to 0$) between smooth surfaces, particles typically have microscopic roughness elements that will touch the opposing surface while the gap between the nominal particle surfaces is non-zero, (ii) *elastohydrodynamic deformation* – if the relative velocity remains large enough when the gap becomes small enough, then the lubrication force exerted by the thin liquid layer will become sufficiently large that it will deform the solid particles in the region of near contact, and the particle will then rebound when the energy of elastic deformation is released and (iii) *glass transition* – for many fluids, the viscosity increases with pressure, and may even undergo a glass transition at large pressure, so that a solid-like collision takes place. The dominant criterion employed in a given situation is typically based on which occurs first (i.e. which has the largest critical separation).

Although the transition from a liquid-mediated interaction of undeformed spheres to solid deformation and then release of this deformation requires time, it is assumed that this process is short compared to the time scale for the relative motion to squeeze the viscous fluid out of the gap separating the sphere surfaces. This assumption is expected to hold for relatively stiff materials, as justified in § 6.4 with quantitative estimates of the time scales involved. Then, the transition is nearly instantaneous, and the collision and rebound process between two wetted spheres has three stages: (i) an initial soft-sphere stage in which the striker sphere moves through the liquid layer toward the target sphere until the gap reaches h_{min}, (ii) a hard-sphere collision that is essentially instantaneous and causes reversal of the relative velocity, multiplied by a dry coefficient of restitution, e_{dry}, once the gap decreases to h_{min} and (iii) a second soft-sphere stage in which the striker sphere rebounds through the liquid layer away from the target sphere and ultimately either is brought to rest within the liquid layer (agglomeration) or escapes the liquid layer (separation). With the simultaneous collision of three wetted spheres, there is an even richer array of interactions and possible outcomes, as described below.

4. Solution method

To reduce the number of parameters, equal spheres are considered, with $a_1 = a_2 = a_3 = 2a$ and $m_1 = m_2 = m_3 = 2m$, where a and m are the reduced radius and mass of a particle pair. The governing equations are then non-dimensionalized, using h_{12}^0 as the length scale, v_1^0 as the velocity scale and h_{12}^0/v_1^0 as the time scale. Combining (2.2) and (2.3) then yields

$$St\frac{\mathrm{d}\hat{v}_{12}}{\mathrm{d}\hat{t}} = -\hat{v}_{12}(1-\hat{h}_{12})^2/\hat{h}_{12} + \frac{1}{2}\hat{v}_{23}(1-\hat{h}_{23}/\hat{h}_{23}^f)^2/\hat{h}_{23}, \tag{4.1a}$$

$$St\frac{\mathrm{d}\hat{v}_{23}}{\mathrm{d}\hat{t}} = -\hat{v}_{23}(1-\hat{h}_{23}/\hat{h}_{23}^f)^2/\hat{h}_{23} + \frac{1}{2}\hat{v}_{12}(1-\hat{h}_{12})^2/\hat{h}_{12}, \tag{4.1b}$$

where $St = mv_1^0/(6\pi\mu a^2)$ is the Stokes number, $\hat{h}_{ij} = h_{ij}/h_{12}^0$, $\hat{v}_{ij} = v_{ij}/v_1^0$, $\hat{t} = tv_1^0/h_{12}^0$ and $\hat{h}_{23}^f = h_{23}^f/h_{12}^0$. It is noted that, if any quantity in parentheses in (4.1) becomes negative, then it is replaced by zero (because the spheres have then separated and the lubrication force is zero). In dimensionless form, the initial conditions become

$$\hat{v}_{12} = 1, \quad \hat{v}_{23} = 0, \quad \hat{h}_{12} = 1, \quad \hat{h}_{23} = \hat{h}_{23}^0 \quad \text{at } \hat{t} = 0, \tag{4.2a–d}$$

where $\hat{h}_{23}^0 = h_{23}^0/h_{12}^0$.

Equations (2.4) and (4.1) are solved numerically (a simple, second-order Runge–Kutta method suffices), starting from the initial conditions. If and when the rebound criterion, $\hat{h}_{ij} = \hat{h}_{min}$ (where $\hat{h}_{min} = h_{min}/h_{12}^0$), is met for either particle pair, then an instantaneous hard-sphere collision is assumed at that time point. Then, using conservation of momentum and the definition of the coefficient of restitution, the relative velocities for equal spheres become

$$v_{ij}^a = -e_{dry}v_{ij}^b, \quad v_{jk}^a = v_{jk}^b + (1+e_{dry})v_{ij}^b/2, \tag{4.3a,b}$$

where e_{dry} is the solid or dry coefficient of restitution and the superscripts 'a' and 'b' refer to immediately after and before the hard-sphere collision, respectively, with i–j the colliding pair and j–k the adjacent pair. In practice, e_{dry} is typically near unity

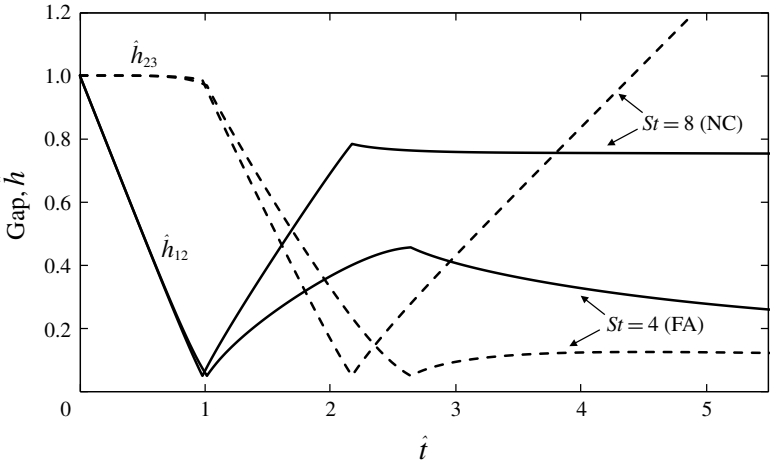

FIGURE 3. Dimensionless separation gaps versus dimensionless time for the simultaneous collision of three wetted spheres that have $e_{dry} = 1$ and equal initial and final separation gaps ($h_{23}^0 = h_{23}^f = h_{12}^0 = h_{12}^f$) and a bounce criterion of $h_{min} = 0.05h_{12}^0$.

for many materials at slow impact speeds (< 0.1 m s^{-1}) and then gradually decreases with increasing impact speed (e.g. Brake, Reu & Aragon 2017; Bordbar & Hyppänen 2007). In the present simulations, a constant or average value of e_{dry} is used for each set of calculations, but it would be simple to use a variable value, if the dependence of e_{dry} on impact speed was known. The simulations are continued until the relative velocities of both pairs reduce to zero (FA), both pairs separate beyond their liquid layers (FS) or one pair separates and the other has zero relative motion (NC or RNC). As will be shown, there are also cases where FS occurs, but is then followed by FA, NC or RNC due to subsequent collisions.

5. Results and discussion

5.1. *Simultaneous collisions*

We first consider $d_{12}^0 = d_{23}^0 = 0$, so that there is simultaneous interaction of all three spheres (that is, the 2–3 collision starts at the same time as the 1–2 collision). Figure 3 shows example results when $\hat{h}_{min} = 0.05$ and $\hat{h}_{23}^0 = \hat{h}_{23}^f = 1$ (meaning the combined liquid-layer thicknesses on the 1–2 and 2–3 pairs are the same). For $St = 4$, the 1–2 gap decreases quickly as sphere 1 approaches sphere 2, until $\hat{t} = 1.01$, when the minimum gap is reached ($\hat{h}_{12} = 0.05$) and rebound occurs. During the initial phase, $\hat{h}_{23}$ decreases only slowly, as spheres 2 and 3 are initially motionless and have considerable inertia that resists motion. However, when the 1–2 collision occurs, the momentum of sphere 1 is transferred to sphere 2. The latter then moves quickly toward sphere 3 and makes contact at $\hat{t} = 2.64$, although with reduced velocity due to viscous losses. Moreover, the relative velocity of the 1–2 pair as it rebounds apart is slowed considerably, not just by tensile lubrication in the 1–2 film resisting this separation but also by compressive lubrication in the 2–3 film resisting the movement of sphere 2 away from sphere 1. The 2–3 pair then bounces slowly apart while particles 1 and 2 again move toward one another due to the reversal of motion of sphere 2. However, neither pair has enough kinetic energy to overcome the viscous losses and separate, so this interaction ends in the fully agglomerated state.

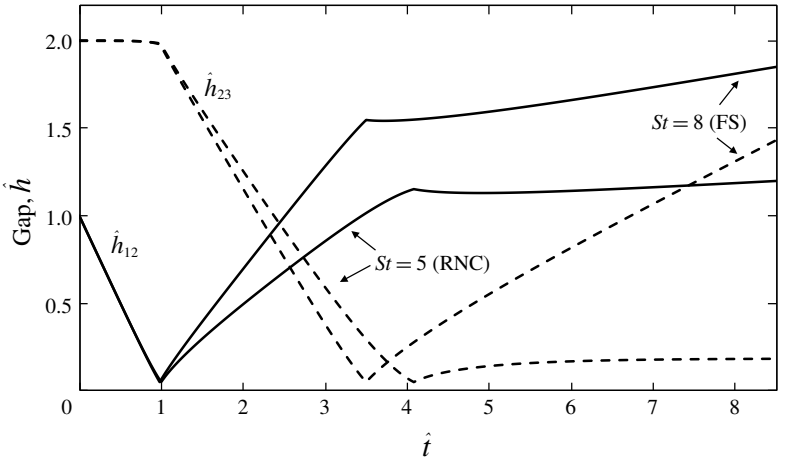

FIGURE 4. Dimensionless separation gaps versus dimensionless time for the simultaneous collision of three wetted spheres with $e_{dry} = 1$, a thicker combined layer on the 2–3 pair ($h^0_{23} = h^f_{23} = 2h^0_{12}$) and a bounce criterion of $h_{min} = 0.05h^0_{12}$.

A different outcome occurs when $St = 8$. There is again collision and rebound of the 1–2 pair (at $\hat{t} = 0.98$), followed by collision and rebound of the 2–3 pair (at $\hat{t} = 2.17$). In this case, rebound of the 2–3 pair is quite strong, and the pair separates ($\hat{h}_{23} > 1$) at $\hat{t} = 4.41$. The 1–2 pair almost separates after its collision and rebound. However, when the 2–3 collision occurs, sphere 2 rebounds back towards sphere 1, so that $\hat{h}_{12}$ no longer increases and the 1–2 pair remains agglomerated. Thus, the outcome is Newton's cradle, with the 1–2 pair remaining together and the third sphere separating after the collision.

If the liquid-layer thicknesses on the 2–3 pair are larger, then rebound of this pair will not be as strong, due to greater viscous dissipation. Figure 4 shows simulation results for the simultaneous collision of three equal spheres but with the combined liquid layer on the 2–3 pair twice as thick as on the 1–2 pair ($\hat{h}^0_{23} = \hat{h}^f_{23} = 2$), again with $\hat{h}_{min} = 0.05$. For $St = 4$ (not shown) the result again is FA. In contrast, the 1–2 pair separates ($\hat{h}_{12} > 1$) after rebound for $St = 5$, while the 2–3 pair remains agglomerated. Thus, this case yields RNC, while $St = 5$ with $\hat{h}^0_{23} = \hat{h}^f_{23} = 1$ still yields FA (not shown). When the Stokes number is increased further for $\hat{h}^0_{23} = \hat{h}^f_{23} = 2$, the spheres have enough inertia to overcome the viscous resistance and fully separate after the collision, as shown in figure 4 for $St = 8$.

A wet coefficient of restitution maybe defined for each pair of spheres,

$$e_{ij} = |v^f_{ij}|/v^0_{12}, \tag{5.1}$$

where v^f_{ij} is the relative velocity of the i–j pair after the collisions (either zero if the pair does not separate, or non-zero if the pair separates). To clarify, v^f_{ij} is the final relative velocity, after the three-sphere interaction is complete. The initial relative velocity of the 1–2 pair, $v^0_{12} = v^0_1$, is used in (5.1) for both the 1–2 and 2–3 pairs, as the initial velocities of spheres 2 and 3 are zero in these simulations.

Figure 5 provides a plot of the coefficients of restitution versus the Stokes number for the conditions of figure 3. For films of equal thickness, only two outcomes are

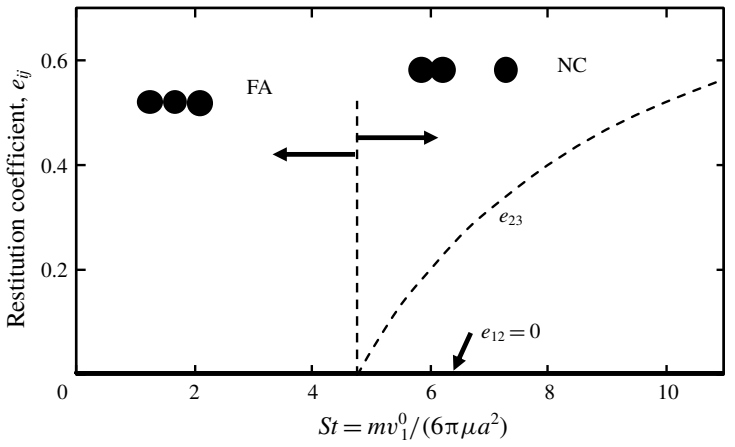

FIGURE 5. Wet coefficients of restitution versus Stokes number for the conditions of figure 3.

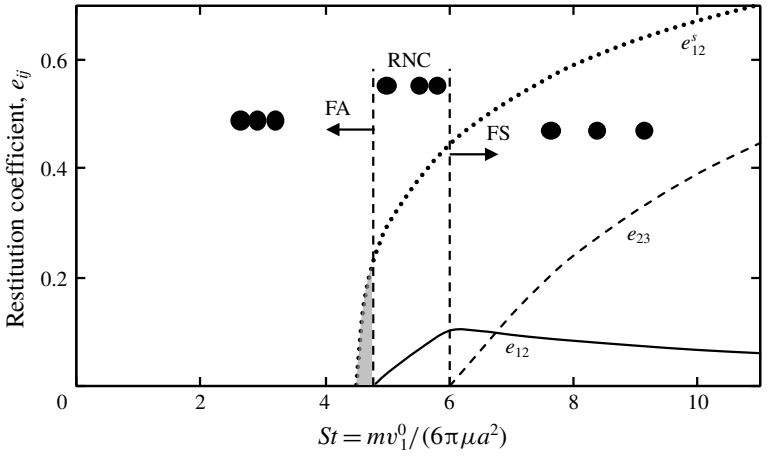

FIGURE 6. Wet coefficients of restitution versus Stokes number for the conditions of figure 4. The dotted line represents an initial or temporary restitution coefficient of the 1–2 pair, immediately after it first separates.

observed: FA and NC. For $St \leqslant 4.8$, all three spheres stick together (FA), due to viscous losses. For $St > 4.8$, the 1–2 pair sticks together, while sphere 3 bounces away as in the conventional Newton's cradle. The velocity at which sphere 3 moves away from the 1–2 pair is reduced by viscous losses, but e_{23} increases with increasing St as inertia becomes more important relative to the viscous forces.

A very different scenario is shown in figure 6, when there is a thicker combined liquid layer on the 2–3 pair. Full agglomeration occurs for $St \leqslant 4.8$. However, for $4.8 < St < 6.0$, reverse Newton's cradle is observed, with sphere 1 bouncing away from the 2–3 agglomerated pair. Then, for $St > 6.0$, full separation of all three spheres is obtained. The shaded region, for $4.55 < St < 4.80$, marks an interesting scenario, not present for two-sphere collisions. In it, sphere 1 initially collides, rebounds and separates ($\hat{h}_{12} > 1$) from sphere 2. Shortly thereafter, sphere 2 collides with sphere 3

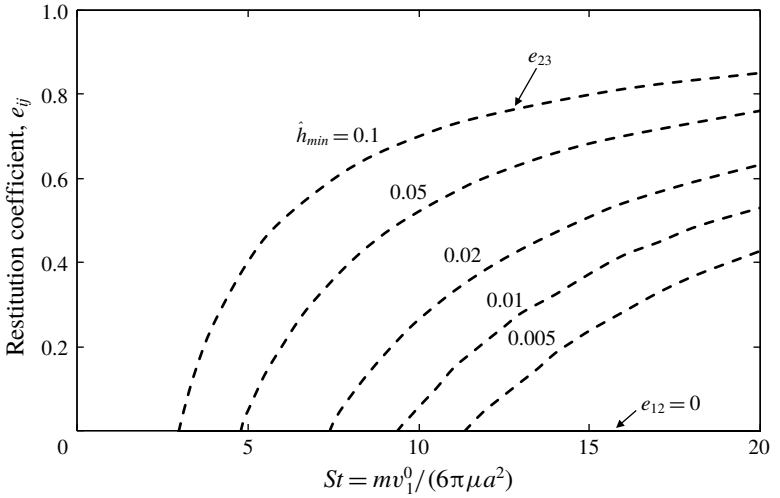

FIGURE 7. Wet coefficients of restitution versus Stokes number for the simultaneous collision of three wetted spheres that have $e_{dry} = 1$, equal initial and final separations gaps ($h_{23}^0 = h_{23}^f = h_{12}^0 = h_{12}^f$) and bounce criteria of $h_{min}/h_{12}^0 = 0.005, 0.01, 0.02, 0.05$ and 0.1.

and partially rebounds. During the 2–3 collision, sphere 1 catches back up with sphere 2, and their liquid layers again overlap ($h_{12} < h_{12}^0$), with the pair remaining agglomerated for this range of Stokes numbers. For $St > 4.8$, sphere 1 remains separated from sphere 2, but e_{12} is substantially reduced by the 2–3 interaction. The dotted line in figure 6 shows e_{12}^s, which is the temporary coefficient of restitution immediately after the 1–2 pair first separates. The much lower solid line is the final value of e_{12}, after the 2–3 interaction. Finally, for $St > 6.0$, the 2–3 pair also has a strong enough collision to rebound and separate, resulting in full separation of all three spheres. Then, e_{23} increases with increasing St, but e_{12} decreases due to stronger rebound of the 2–3 pair. This behaviour of e_{12} and e_{23} crossing was observed by Donahue *et al.* (2010*b*) in experiments with a pre-existing liquid bridge, so that the final film thickness on the 2–3 pair was relatively large.

Figure 7 shows the coefficients of wet restitution for simultaneous three-sphere collisions in which the initial and final liquid-layer thicknesses are the same for both pairs, but with various values of the minimum separation at which contact and bounce occur. As also seen in figure 5, the only outcomes are full agglomeration (FA, $e_{12} = e_{23} = 0$) for Stokes numbers below a critical value, and Newton's cradle (NC, $e_{12} = 0$, $e_{23} > 0$) for Stokes numbers above the critical value. The critical Stokes number is larger, and the 2–3 rebound velocity is lower, for smaller values of the minimum gap, due to the greater viscous dissipation when a deeper penetration into the liquid layer is required for rebound.

Figure 8 shows an outcomes map for the simultaneous collision of three spheres, when the 2–3 pair has initial and final liquid-layer thicknesses twice that of the 1–2 pair. In this case, full agglomeration (FA, $e_{12} = e_{23} = 0$) is predicted for small Stokes numbers, reverse Newton's cradle (RNC, $e_{12} > 0, e_{23} = 0$) is predicted for intermediate Stokes numbers and full separation (FS, $e_{12} > 0, e_{23} > 0$) is predicted for large Stokes numbers. The range of Stokes numbers for RNC has a nearly constant, small span as the minimum gap is increased, but shifts toward lower Stokes numbers due to reduced

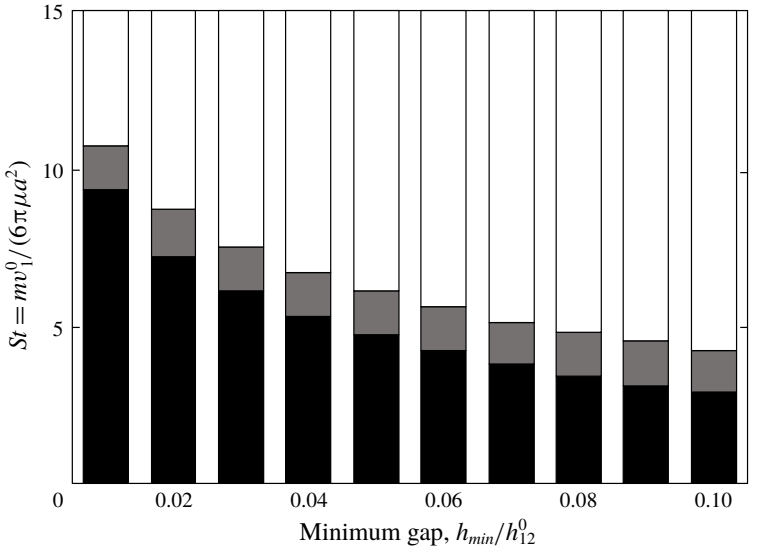

FIGURE 8. Outcomes map of Stokes number versus minimum gap for simultaneous collision of three wetted spheres with a 2× thicker combined layer on the 2–3 pair than on the 1–2 pair. Three outcomes were observed: FA (■), RNC (■), FS (□).

viscous dissipation. The different set of outcomes for this case compared to that of figure 7 shows both quantitative and qualitative sensitivity to the relative thickness of the liquid layers.

5.2. *Pairwise sequential collisions*

In this subsection, we consider $d_{23}^0 > 0$, so that there is an initial air gap between the liquid layers of spheres 2 and 3. Of most relevance, the 2–3 collision is then initiated after the 1–2 collision has started (and maybe even finished). Figure 9 shows a repeat of the simulations in figure 3, but with $d_{23}^0 = h_{23}^0 = h_{12}^0$ (so that the initial air gap is of the same thickness as the combined liquid film). The result for $St = 4$ is the same (FA) as when $d_{23}^0 = 0$, but it takes longer before the 2–3 collision occurs (at $\hat{t} = 4.31$ versus 2.64) and arrests the separation of the 1–2 pair. The result for $St = 8$ is different (FS versus NC), however, because the 1–2 pair bounces and separates before the 2–3 pair collides (at $\hat{t} = 3.42$ versus 2.71), with the delay in the 2–3 collision due to the time required for sphere 2 to move across the air gap between it and sphere 3. In what follows, we first consider the latter case, with sequential pairwise collisions. The former case, when the 2–3 collision is initiated before the 1–2 collision is complete, is considered in § 5.3.

Collision of 1–2 pair – if the initial air gap between spheres 2 and 3 is large enough, then the 1–2 pair may collide and bounce apart before encountering the third particle. Since the collisions are then pairwise, the analysis is simplified and yields analytical results. Considering first the 1–2 collision, equation (4.1*a*) becomes

$$St\frac{\mathrm{d}\hat{v}_{12}}{\mathrm{d}\hat{t}} = -\hat{v}_{12}(1-\hat{h}_{12})^2/\hat{h}_{12}. \tag{5.2}$$

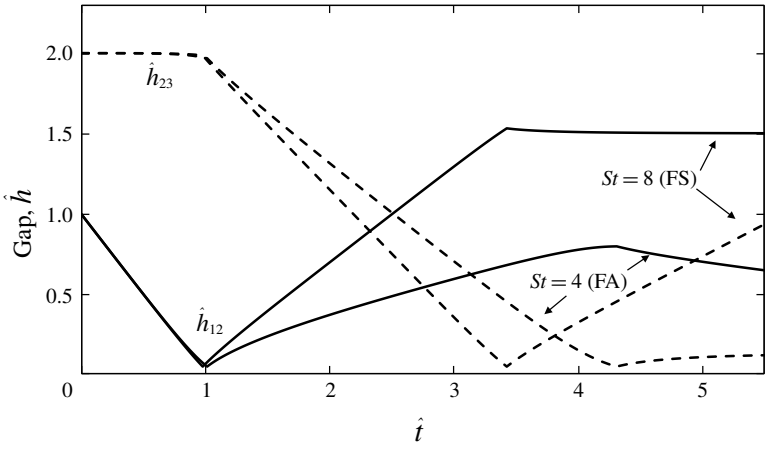

FIGURE 9. Dimensionless separation gaps versus dimensionless time for the sequential collisions of three wetted spheres with $e_{dry} = 1$, equal initial and final film thicknesses, an initial air gap of $d_{23}^0 = h_{12}^0$ and a bounce criterion of $h_{min} = 0.05h_{12}^0$.

Dividing (5.2) by (2.4) to eliminate time yields

$$St\frac{\mathrm{d}\hat{v}_{12}}{\mathrm{d}\hat{h}_{12}} = (1-\hat{h}_{12})^2/\hat{h}_{12}. \tag{5.3}$$

Using the initial condition $\hat{v}_{12} = 1$ when $\hat{h}_{12} = 1$, equation (5.3) may be integrated to give

$$St(1-\hat{v}_{12}) = (1-\hat{h}_{12}^2)/2 - 2(1-\hat{h}_{12}) - \ln\hat{h}_{12} \tag{5.4}$$

for the approach stage of the collision.

In order for the 1–2 pair to bounce apart, the gap must first decrease to h_{min} during approach, and then increase back to h_{12}^0 during rebound. For contact ($h_{12} = h_{min}$) to occur, it is necessary that $v_{12} > 0$ when $h_{12} = h_{min}$, which requires $St > St_c$, where

$$St_c = (1-\hat{h}_{min}^2)/2 - 2(1-\hat{h}_{min}) + \ln(1/\hat{h}_{min}) \tag{5.5}$$

is the critical stokes number for contact. The dimensionless contact time, $\hat{t}_c$, is determined by integrating the dimensionless form of (2.4) from $\hat{h}_{12} = 1$ at $t = 0$ to $\hat{h}_{12} = \hat{h}_{min}$ at $\hat{t} = \hat{t}_c$, using (5.4) for the relative dimensionless velocity,

$$\hat{t}_c = \int_{\hat{h}_{min}}^{1} \frac{\mathrm{d}\hat{h}}{1-(\ln(1/\hat{h}) - 2(1-\hat{h}) + (1-\hat{h}^2)/2)/St}. \tag{5.6}$$

Upon contact for $St > St_c$ the relative velocity changes sign, and the 1–2 pair bounces apart, starting from $\hat{h}_{12} = \hat{h}_{min}$ and

$$\hat{v}_{12} = \hat{v}_{12}^a = -e_{dry}\hat{v}_{12}^b = -e_{dry}(1 - St_c/St), \tag{5.7}$$

where $\hat{v}_{12}^b$ and $\hat{v}_{12}^a$ are the relative velocities just before and after contact occurs, respectively. Then, equation (5.3) may be integrated subject to this initial condition to give

$$St(\hat{v}_{12} - \hat{v}_{12}^a) = \ln(\hat{h}_{12}/\hat{h}_{min}) - 2(\hat{h}_{12} - \hat{h}_{min}) + (\hat{h}_{12}^2 - \hat{h}_{min}^2)/2 \tag{5.8}$$

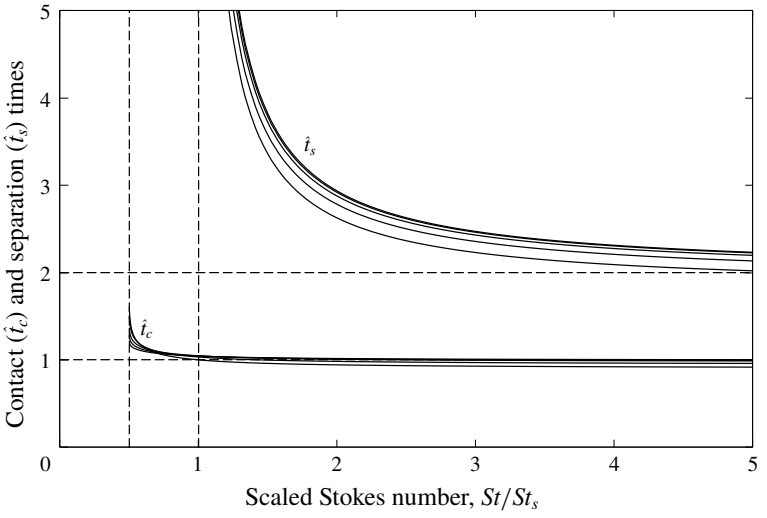

FIGURE 10. Dimensionless contact and separation times versus the Stokes number scaled with the minimum Stokes number for rebound and separation for the collision of two perfectly elastic spheres ($e_{dry} = 1$) covered with a thin layer of viscous liquid. The different curves are for $\hat{h}_{min} = 0.005$, 0.01, 0.02, 0.05 and 0.1 (bottom to top for $\hat{t}_c$ near $St/St_s = 0.5$, then crossing for larger St/St_s, and top to bottom for $\hat{t}_s$).

during the rebound stage. Separation of the 1–2 sphere will occur if the magnitude of v_{12} does not decline to zero by the time that $\hat{h}_{12} = 1$ is reached, which requires $St > St_s$, where

$$St_s = St_c(1 + e_{dry})/e_{dry} \tag{5.9}$$

is the critical Stokes number for separation. The dimensionless separation time is then found by integrating (2.4) from $\hat{h}_{12} = \hat{h}_{min}$ at $\hat{t} = \hat{t}_c$ to $\hat{h}_{12} = 1$ at $\hat{t} = \hat{t}_s$ using (5.8) for the relative velocity, along with (5.5), (5.7) and (5.9),

$$\hat{t}_s = \hat{t}_c + \int_{\hat{h}_{min}}^{1} \frac{\mathrm{d}\hat{h}}{e_{dry}(1 - St_s/St) + (\ln(1/\hat{h}) - 2(1 - \hat{h}) + (1 - \hat{h}^2)/2)St}. \tag{5.10}$$

Figure 10 shows plots of $\hat{t}_c$ and $\hat{t}_s$ versus the Stokes number (normalized by St_s, so that the curves nearly collapse) for various values of the minimum gap, assuming perfectly elastic solid–solid contacts ($e_{dry} = 1$) where $St_s = 2St_c$. For large St ($St \gg St_s$), $\hat{t}_c \approx 1 - \hat{h}_{min}$ and $\hat{t}_s \approx 2 - 2\hat{h}_{min}$, as there is sufficient inertia that the relative velocity is not significantly reduced in magnitude as the striker sphere penetrates the liquid film, hits the target sphere and then rebounds. In contrast, for St only slightly greater than St_c and St_s, $\hat{t}_c$ and especially $\hat{t}_s$, respectively, are larger due to the viscous resistance slowing down the approach and rebound. Note that there is a weak singularity in the contact time, $\hat{t}_c = O(\ln(1/(St - St_c)))$, and a strong singularity in the separation time, $\hat{t}_s = O(1/(St - St_s))$, near the critical Stokes number for contact and separation, respectively.

Moreover, the relative velocity for separation, $\hat{v}_{12}^s$, is given by (5.8) with $\hat{h}_{12} = 1$, which allows for the wet coefficient of restitution to be determined,

$$e_{12} = |\hat{v}_{12}^s| = -v_{12}^s/v_1^0 = e_{dry}(1 - St_s/St). \tag{5.11}$$

Of course, equation (5.11) only applies if $St > St_s$ as given by (5.5) and (4.2). When $St \leqslant St_s$ the colliding spheres do not have enough inertia to overcome the viscous losses and so the 1–2 pair remains agglomerated ($e_{12} = 0$). Also, capillary forces would come into play for $St \approx St_s$, which would cause a small increase in the critical Stokes number required to overcome both lubrication and capillary forces and thereby allow separation.

Collision of 2–3 pair – we next consider the 2–3 pair, so that we can determine its collision profile and also the conditions required for the 1–2 pair to separate prior to the 2–3 pair interacting. At the time t_s, when the 1–2 pair separates, sphere 2 has travelled a distance $v_1^0 t_s/2$, or $\hat{t}_s/2$ in dimensionless terms. This result follows from the fact that the centre of mass of the 1–2 pair necessarily moves at constant velocity $v_1^0/2$ (due to conservation of momentum), and that the centre of sphere 2 is at a distance $a_2 + \delta_{12}/2$ from the centre of mass at both $t = 0$ and $t = t_s$. Thus, the criterion for the 1–2 pair interaction to be completed before the 2–3 pair interaction begins is simply

$$d_{23}^0 > v_1^0 t_s/2, \quad \text{or} \quad \hat{d}_{23}^0 > 0.5\hat{t}_s. \tag{5.12a,b}$$

If this criterion is met, then sphere 2 will have separated from sphere 1 before striking sphere 3, and so we have sequential pairwise collisions. Since $v_1 + v_2 = v_1^0$ (from conservation of momentum) and $v_2 - v_1 = e_{dry}(1 - St_s/St)v_1^0$ from (5.11), upon separation of the 1–2 pair and prior to contact of the 2–3 sphere, the individual sphere velocities are

$$v_1^s = v_1^0(1 - e_{dry}(1 - St_s/St))/2, \quad v_2^s = v_1^0(1 + e_{dry}(1 - St_s/St))/2, \quad v_3^s = 0. \tag{5.13a–c}$$

Using these initial conditions, the 2–3 collision proceeds with a similar description as above for the 1–2 collision. There is a caveat, however. Sphere 2 is slowed when it collides with sphere 3, presenting the possibility that sphere 1 catches back up and hits the 2–3 pair! To check this scenario, note that conservation of momentum requires that $(v_2 + v_3)/2 = v_1^0(1 + e_{dry}(1 - St_s/St))/4$. On average, from when the 2–3 liquid films first touch until they separate, sphere 2 has this speed (assuming $h_{23}^f = h_{23}^0$). Sphere 1 can then catch up with the 2–3 pair only if v_1 from (5.13) exceeds this value, which requires that

$$St < 3e_{dry}St_s/(3e_{dry} - 1), \quad \text{or} \quad St < 3St_c/2 \quad \text{for } e_{dry} = 1. \tag{5.14a,b}$$

Since $St > St_s$ is required for the 1–2 pair to bounce and separate, (5.14) shows that the range of allowing for sphere 1 to catch up to the 2–3 pair is quite narrow for $e_{dry} \approx 1$ (as was seen in figure 5). The range becomes larger when e_{dry} is reduced, because the velocity of sphere 2 after separation is reduced while that of sphere 1 is increased. For $e_{dry} \leqslant 1/3$, sphere 1 has a larger velocity than does the 2–3 pair for all $St > St_s$. Of course, whether or not sphere 1 catches and collides with the 2–3 pair depends on the initial separation and the duration of the 2–3 collision, as described later.

If (5.12) is met, the 1–2 pair separates before encountering the third sphere. Sphere 2 then travels at the speed v_2^s given by (5.13) and encounters the third sphere at time t_{23},

$$t_{23} = t_s + (2d_{23}^0 - v_1^0 t_s)/v_2^s. \tag{5.15}$$

Assuming that the initial separation is large enough that sphere 1 does not catch the 2–3 pair, the 2–3 collision is then described by the same analysis as for the

1–2 collision, except that the impact velocity is given by v_2^s from (5.13) instead of v_1^0, and the initial film thickness is given by h_{23}^0 instead of h_{12}^0. It is assumed that the final film thickness for separation is the same as the initial film thickness, $h_{23}^f = h_{23}^0$, because there would not be excess fluid in the 2–3 gap if the spheres initially are separated. A modified Stokes number, $St^* = mv_2^s/(6\pi\mu a^2)$ and a modified dimensionless minimum separation, $h_{min}^* = h_{min}/h_{23}^0$, are defined as governing parameters for the 2–3 collision. The critical Stokes number for separation is then

$$St_s^* = [\ln(1/h_{min}^*) - 2(1 - h_{min}^*) + (1 - (h_{min}^*)^2)/2](1 + e_{dry})/e_{dry}, \tag{5.16}$$

where the 2–3 pair will bounce and separate only if $St^* > St_s^*$. Note from (5.13) that

$$St^* = (St(1 + e_{dry}) - e_{dry}St_s)/2. \tag{5.17}$$

Moreover, for equal film thicknesses ($h_{23}^0 = h_{12}^0$), combining (5.5), (5.9) and (5.16) yields $St_s^* = St_s$. Then, $St^* > St_s^*$ is equivalent to

$$St > St_s(2 + e_{dry})/(1 + e_{dry}), \quad \text{if } h_{23}^0 = h_{12}^0, \tag{5.18}$$

for the isolated 2–3 pair to separate. Now, comparing (5.14) and (5.18), it is seen that sphere 1 is only able to catch up to the 2–3 pair for $e_{dry} = 1$ under conditions for which the pair remains agglomerated ($St < 3St_s/2$). For $e_{dry} < 1$, however, there is a window for which sequential pairwise collisions are possible,

$$(2 + e_{dry})/(1 + e_{dry}) < St/St_s < 3e_{dry}/(3e_{dry} - 1), \tag{5.19}$$

where St_s is given by (5.5) and (5.9).

When $St^* > St_s^*$, an isolated 2–3 pair will eventually bounce apart, with a wet coefficient of restitution of

$$e_{23}^* = -v_{23}^s/v_2^s = e_{dry}(1 - St_s^*/St^*), \quad \text{or} \tag{5.20a}$$

$$e_{23} = -v_{23}^s/v_1^0 = e_{dry}(1 - St_s^*/St^*)(1 + e_{dry}(1 - St_s/St))/2, \quad \text{or} \tag{5.20b}$$

$$e_{23} = \frac{e_{dry}}{2}\left[1 + e_{dry}(1 - St_s/St) - 2St_s/St\right], \quad \text{if } h_{23}^0 = h_{12}^0. \tag{5.20c}$$

And, the duration of the 2–3 collision (from when the liquid films first overlap until they separate) is t_s^*, given by (5.6) and (5.10) but with St^*, St_s^* and h_{min}^* replacing St, St_s and $\hat{h}_{min}$, respectively; here, $t^* = v_2^s t/h_{23}^0$ is the modified dimensionless time.

Figure 11 shows the wet coefficient of restitution for the 1–2 pair from (5.11) and for the 2–3 pair from (5.20*c*) for various values of e_{dry}. Both coefficients are zero for Stokes numbers below the critical value for separation ($St < St_s$ for the 1–2 pair, and $St < St_s(2 + e_{dry})/(1 + e_{dry})$ for the 2–3 pair) and then increase toward e_{dry} as the Stokes number increases. The critical value for rebound of the 1–2 pair, St_s, increases with decreasing minimum gap and dry coefficient of restitution, as given by (5.5) and (5.9). The critical Stokes number for rebound of the 2–3 pair increases even further with decreasing dry coefficient of restitution, as given by (5.16).

5.3. *Non-pairwise sequential collisions*

We can now determine if sphere 1 will catch back up to the 2–3 pair before it separates. In this case, the sequential 1–2 and 2–3 collisions are not solely pairwise.

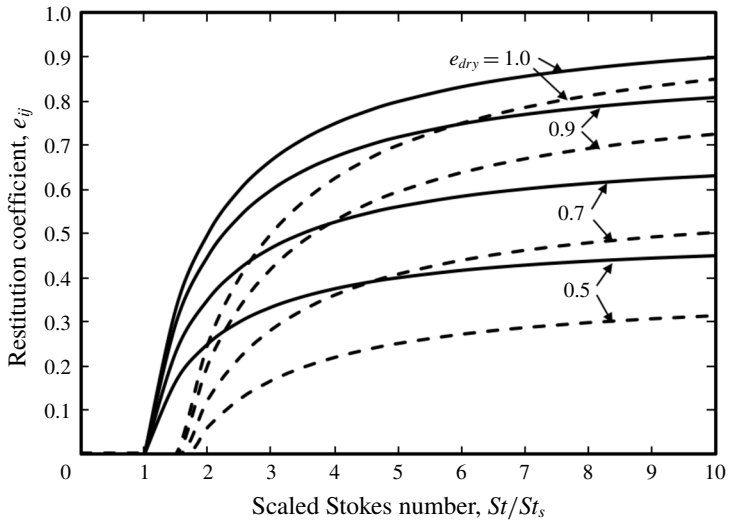

FIGURE 11. Coefficient of wet restitution versus the scaled Stokes number for different values of the dry restitution coefficient ($e_{dry} = 0.5$, 0.7, 0.9 and 1.0). The solid curves are for the 1–2 pair, and the dashed curves are for the 2–3 pair. It is assumed that the initial separation is large, so that there are sequential pairwise collisions; the values of e_{23} are for equal film thicknesses: $h_{23}^f = h_{23}^0 = h_{12}^0$.

Sphere 2 travels a distance of $v_2^s(h_{23}^0 t_s^*/v_2^s)/2$ from the time it first encounters sphere 3 until this pair separates. During this time, sphere 1 travels a distance $v_1^s(h_{23}^0 t_s^*/v_2^s)$, but it starts at a distance $(d_{23}^0 - v_1^0 t_s/2)(1 - v_1^s/v_2^s)$ separating its liquid layer from that of sphere 2 when the 2–3 encounter begins. Thus, the criterion for sphere 1 to collide with the 2–3 pair is

$$d_{23}^0 < h_{23}^0 t_s^*(v_1^s/v_2^s - 1/2)/(1 - v_1^s/v_2^s) + h_{12}^0 \hat{t}_s/2. \tag{5.21}$$

If d_{23}^0 is instead larger than the right-hand side of (5.21), and with $St^* > St_s^*$, then the 2–3 pair bounces and separates before sphere 1 collides again with sphere 2.

These concepts are illustrated in figure 12, which presents a regime map or 'phase diagram' for $\hat{d}_{23}^0$ versus St/St_s for $\hat{h}_{min} = 0.05$, equal layer thicknesses and various values of e_{dry}. There are several noteworthy features.

(i) For $St/St_s < 1$, the 1–2 pair remains agglomerated and eventually strikes sphere 3, even for large initial separations, resulting in full agglomeration of the triplet.

(ii) For $e_{dry} = 1$, there is a single branch, $\hat{d}_{23}^0 = 0.5\hat{t}_s$ below which sphere 1 catches the 2–3 pair for a second time and above which it does not.

(iii) For $e_{dry} < 1$, there is a second branch, $\hat{d}_{23}^0 = t_s^*(v_1^s/v_2^s - 0.5)/(v_1^s/v_2^s - 1) + 0.5\hat{t}_s$, above which the 2–3 pair rebounds and separates before sphere 1 catches it again.

(iv) The two branches co-exist only in the window of St given by (5.19), and between these branches sphere 1 catches back up and collides with the 2–3 pair before it can separate.

(v) For $St > St_s$, the ultimate outcome depends on the Stokes number and other parameters.

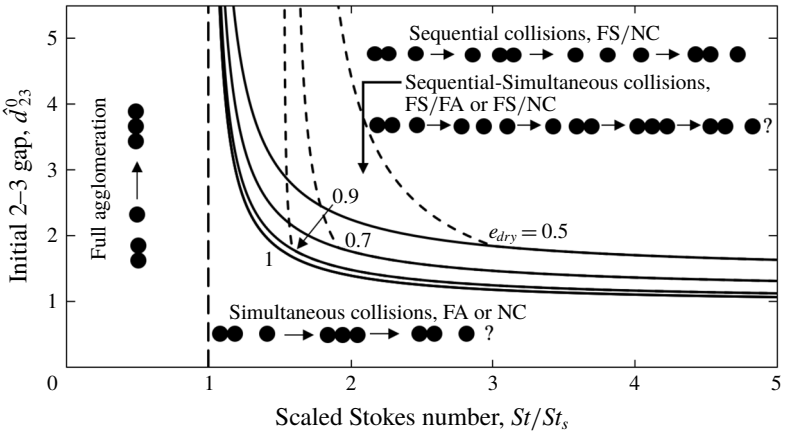

FIGURE 12. Regime map of initial air gap between the 2–3 pair versus the scaled Stokes number for $h_{min} = 0.05h_{12}^0$, equal liquid layers ($h_{23}^f = h_{23}^0 = h_{12}^0$) and various dry coefficients of restitution ($e_{dry} = 1.0$, 0.9, 0.1 and 0.5, from left to right). The solid lines are given by (5.12) and the dashed lines by (5.21).

As seen above, pairwise sequential collisions occur only when both conditions $St > St_s$ and $d_{23}^0 > h_{23}^0 t_s^*(v_1^s/v_2^s - 1/2)/(v_1^s/v_2^s - 1) + h_{12}^0 \hat{t}_s/2$ are met. For $St < St_s$, the 1–2 pair remains agglomerated indefinitely and so eventually traverses the d_{23}^0 gap and then encounters sphere 3 in a ternary collision. In contrast, when St/St_s and (5.21) is satisfied, the 1–2 pair separates but then sphere 1 collides again with sphere 2 when it is still agglomerated with sphere 3. Figure 13 illustrates these different outcomes for $\hat{h}_{min} = 0.05$, $e_{dry} = 0.5$ and a dimensionless initial air gap of $\hat{d}_{12}^0 = 3$. Under these conditions, $St_s = 4.78$, the first branch is at $St/St_s = 1.50$, and the second branch is at $St/St_s = 2.27$. When $St = 6$, $St/St_s < 1.50$, and the 2–3 pair collides and begins to separate before the 1–2 pair is able to separate, and so full agglomeration results ($\hat{h}_{12} < 1$ and $\hat{h}_{23} < 1$). For $St = 8$, $1.50 < St/St_s < 2.27$, and the 1–2 pair separates before the 2–3 collision begins. However, once the gap between the 2–3 pair reaches h_{min} and the spheres begin to rebound, the 1–2 separation decreases and so full agglomeration is again the ultimate outcome. This behaviour is denoted as FS/FA, as a full separation occurs after the 1–2 collision but before the 2–3 collision and full agglomeration. For $St = 10$, we again have $1.50 < St/St_s < 2.27$ and the 1–2 pair re-agglomerates after the 2–3 pair begins to separate. For this St, however, the 2–3 pair has sufficient inertia to separate after collision; the ultimate outcome is then Newton's cradle. Similar behaviour, but with a more rapid separation of the 2–3 pair occurs for $St = 12$ and 16, for which $St > 2.27St_s$. This new behaviour is termed FS/NC, as the 2–3 pair separates before the 1–2 pair collides for a second time when $St > 2.27St_s$, and so there is a period of full separation before the final outcome of Newton's cradle.

5.4. *Outcomes maps for sequential collisions*

An outcomes map for sequential collisions is provided in figure 14. Here, equal liquid-layer thicknesses and $\hat{h}_{min} = 0.05$ are again assumed, but with $e_{dry} = 0.9$. In this case, the critical Stokes number for pairwise rebound and separation is $St_s = 3.37$. From (5.19), the window in which pairwise sequential collisions are possible is

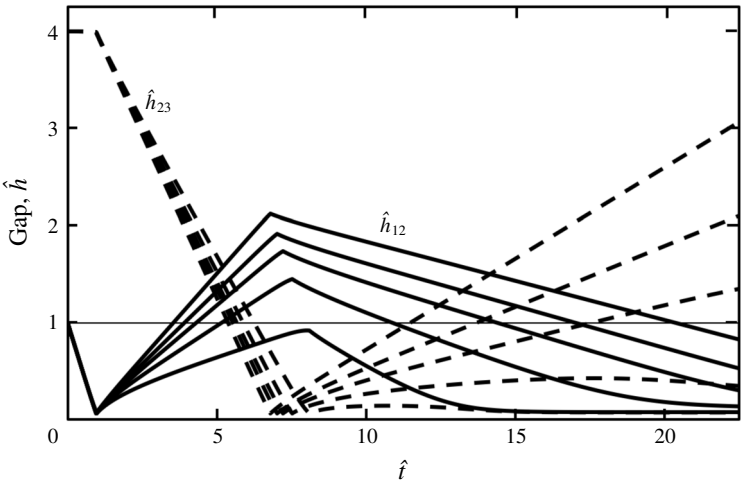

FIGURE 13. Dimensionless separation gaps versus dimensionless time for the sequential collisions of three wetted spheres with equal liquid-layer thicknesses ($h_{23}^f = h_{23}^0 = h_{12}^0$), initial air gap of $d_{23}^0 = 3h_{12}^0$, minimum separation for rebound of $h_{min} = 0.05h_{12}^0$, dry restitution coefficient $e_{dry} = 0.5$ and $St = 6$, 8, 10, 12 and 16 (bottom to top on right-hand side of figure). Separation occurs when the dimensionless gap exceeds unity (horizontal line).

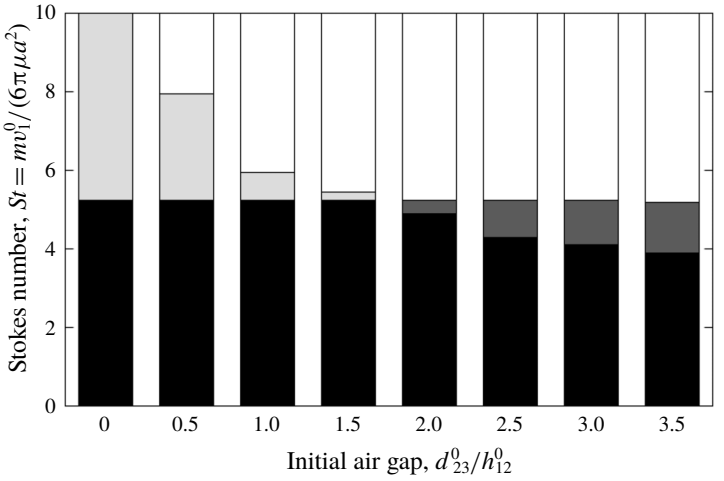

FIGURE 14. Outcomes map of Stokes number versus the initial air gap between the 2–3 pair for sequential collisions of three wetted spheres with $h_{min} = 0.05h_{12}^0$, $e_{dry} = 0.9$ and equal liquid-layer thicknesses ($h_{23}^f = h_{23}^0 = h_{12}^0$). Four outcomes were observed: FA (■), FS/FA (■), NC (■), FS/NC (□).

extremely narrow: $5.14 < St < 5.35$. For smaller St, full agglomeration is always the ultimate outcome of the simulations, though for $\hat{d}_{23}^0 > 1.88$ (where the two branches in figure 12 separate) there is a narrow range of St that yields FS/FA due to temporary separation of the 1–2 pair before collision with the third sphere. For larger St, Newton's cradle is the ultimate outcome of the collisions, although

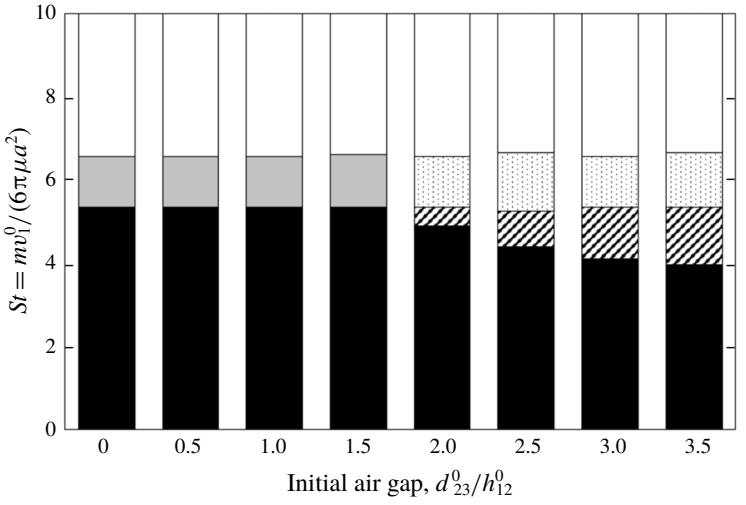

FIGURE 15. Outcomes map of Stokes number versus the initial air gap between the 2–3 pair for sequential collisions of three wetted spheres with $h_{min} = 0.05h_{12}^0$, $e_{dry} = 0.9$ and unequal liquid-layer thicknesses ($h_{23}^f = h_{23}^0 = 2h_{12}^0$). Five outcomes were observed: FA (black), FS/FA (diagonal), RNC (grey), FS/RNC (dotted), FS (white).

FS/NC is observed for the larger St and non-zero $\hat{d}_{23}^0$ as there is then a period of full separation after the initial 1–2 collision and rebound but before the final 1–2 collision and agglomeration.

Figure 14 is for liquid films of equal thickness, and the ultimate outcome is FA for $St < 5.35$ and NC for $St > 5.35$. A very different set of outcomes is achieved for a thicker film on the 2–3 pair, as shown in figure 15. When $h_{23}^f = h_{23}^0 = 2h_{12}^0$, still with $h_{min} = 0.05h_{12}^0$ and $e_{dry} = 0.9$, FA is again the ultimate outcome for $St < 5.35$, but now RNC occurs for $5.35 < St < 6.55$ and then FS for $St > 6.55$. The initial 2–3 air gap does not have a significant impact on the final outcome, but a gap of $d_{23}^0 > 1.8h_{12}^0$ allows for FS prior to the ultimate outcome.

6. Additional considerations

The current work has several assumptions or restrictions, which may be of practical importance in physical systems. These issues include (at least) the role of capillary forces, the possibility of cavitation during rebound, and the criterion selected for rebound. Each of these issues is discussed below, not as a full analysis but rather to point to considerations for future research.

6.1. *Capillary forces*

A good discussion of capillary forces is provided by Buck *et al.* (2018). They include both a direct contribution from surface tension and an indirect contribution from capillary pressure in the liquid bridge between two wetted spheres. Both of these effects act in the normal direction, typically inward along the line of centres between two spheres, and so aid in the approach stage and resist the rebound stage. For a thin liquid layer, the capillary pressure force dominates and is of order $F_c \approx 2\pi a\sigma$. The viscous lubrication force scales as $F_v \approx 6\pi\mu a^2 v_r/h$, from (2.2), where v_r is the

relative velocity and h the separation gap. Thus, $F_v/F_c \approx Ca = 3\mu a v_r/(h\sigma)$. As an example, consider $\mu = 0.01$ g cm^{-1} s, $\sigma = 73$ g s^{-2} (water in air), $h/a = 0.01$ and $v_r = 100$ cm s^{-1}. Then, $Ca \approx 4$, indicating that viscous forces are larger than capillary forces but perhaps not dominant as assumed in the current work. For more viscous fluids, such as the oil used by Donahue *et al.* (2010*a*,*b*) or liquid polymers, $Ca > 1000$ and viscous forces are expected to dominate. However, for water or other low-viscosity liquids and larger values of h/a, such as employed by Buck *et al.* (2018), capillary forces may be comparable to viscous forces. Indeed, Buck *et al.* (2018) calculated dissipative energies for collisions of glass particles with water layers of thickness approximately 20 % of the particle diameter, and found comparable capillary and viscous effects with collision velocities of about 1 m s^{-1}, but with viscous effects becoming more important with increasing impact velocity.

Of further note is that the relative velocity during rebound can become small near the critical condition for separation: $St = St_s$. Then, capillary forces would become important during the final stages of rebound, even if they are negligible in the initial stages of the collision process. Donahue *et al.* (2012*a*,*b*) investigated an interesting twist on this issue by considering oblique collisions of two wetted particles at large capillary numbers and subcritical Stokes numbers. Then, the colliding pair initially agglomerated and rotated as a doublet, with capillary forces as well as viscous forces playing a role in determining whether or not the rotating doublet would subsequently de-agglomerate due to centrifugal forces.

6.2. *Cavitation*

During the approach stage of collision, the pressure that builds up in the intervening liquid layer is positive and slows the approach. During the rebound stage, however, the dynamic pressure is negative and draws fluid back into the gap between the receding surfaces of the two spheres. If the absolute pressure drops below the vapour pressure of the liquid, then cavitation bubbles may form. Indeed, Marston *et al.* (2011) observed cavitation during the rebound of a sphere from a wetted surface and presented high-speed photographs of the cavitation structure for different fluids and conditions. The possibility of cavitation may be determined from the maximum dynamic pressure. From lubrication theory (Kantak & Davis 2006) the maximum dynamic pressure is along the line of centres and equal to

$$p_d = 3\mu a v_r (1 - (h/h_0)^2)/h^2, \tag{6.1}$$

where h is the instantaneous distance between the sphere surface and $h_0 = h_{12}^0$ is the fluid-layer thickness. When $St \gg St_c$, so that there is strong rebound, $v_r \approx -e_{dry} v_{12}^0$ just after velocity reversal, and $|p_d|$ is maximum when $h = h_{min}$. For typical conditions of $h_0 = 100$ μm, $h = 3$ μm, $|v_r| = 1$ m s^{-1}, $a = 10^{-3}$ m and $\mu = 10^{-3}$ kg (m s^{-1}) (water), $|p_d| \approx 3 \times 10^5$ kg m^{-2} (approximately 3 atm). Thus, cavitation is a realistic consideration and would be even more important for higher impact velocities, larger spheres or more viscous fluids.

As a result of estimates like the one above, early models assumed that cavitation occurred during rebound and neglected or partially neglected viscous resistance during the rebound stage (Barnocky & Davis 1988; Davis *et al.* 2002; Kantak & Davis 2006). However, the more recent study by Donahue *et al.* (2010*a*) demonstrated via modelling and experiment that the fluid resistance during the rebound stage cannot be completely neglected due to presumed cavitation. Moreover, the experiments of Marston *et al.* (2011) support this view, by showing images in which the cavitation

microstructure is quite complex, indicating that it would still impart substantial lubrication resistance. Thus, recent comparisons between theory and experiment on collisions between particles and a wet surface (e.g. Cruger *et al.* 2016; Buck *et al.* 2018), or between two wet particles (Donahue *et al.* 2012*a*), neglect the effects of cavitation on the viscous lubrication resistance during rebound, but they typically match the critical Stokes number for separation, St_s, or some related quantity, to the experimental results as a fitting parameter, since h_{min} is often not known (or only known as an approximation).

6.3. *Rebound criteria*

In the current work, a relatively simple rebound criterion has been employed. Namely, when the nominal separation distance between two colliding surfaces is reduced to h_{min}, the spheres are assumed to have made contact, and their relative velocity is instantly reversed and multiplied by e_{dry}. This criterion is consistent with the view that (Barnocky & Davis 1988; Ma *et al.* 2016)

$$h_{min} = h_b, \tag{6.2}$$

where h_b is the minimum bump or roughness height on the sphere surfaces that could arrest the relative motion (i.e. support the required contact force). The dimensionless minimum separation, $\hat{h}_{min} = h_{min}/h_{12}^0$, may then be varied independently of the Stokes number simply by varying the film thickness, h_{12}^0.

Previous work has explored two other reversal criteria, as summarized by Donahue *et al.* (2010*b*). The first is from the elastohydrodynamic collision theory first proposed by Davis *et al.* (1986),

$$h_{min} = h_e = (3\pi\theta\mu a^{3/2} v_r/\sqrt{2})^{2/5}, \tag{6.3}$$

where $\theta = 2(1-\nu^2)/(\pi E)$, $\nu =$ Poisson's ratio, $E =$ Young's modulus of the colliding spheres. In the original theory, the elastic deformation and release occur gradually due to dynamic lubrication pressure in a soft-sphere collision. For the current criterion, however, they are assumed to occur instantaneously in a hard-sphere collision at the point when the nominal separation between the surfaces decreases to the elastic length scale given by (6.3).

The other reversal criterion is based on the glass transition, in which the liquid film becomes solid like when the dynamic lubrication pressure reaches a glass-transition pressure, p_{gt}. Then, using (6.1) with $h \ll h_0$, this rebound criterion becomes

$$h_{min} = h_g = (3\mu a v_r/p_{gt})^{1/2}. \tag{6.4}$$

Again, this criterion is applied instantaneously (Donahue *et al.* 2010*b*), though a more complete consideration involves a soft-sphere collision using elastohydrodynamic theory coupled with a pressure-dependent viscosity increase (Barnocky & Davis 1989).

The rebound criterion is selected as the largest of h_b, h_e and h_g in a given situation. For the experiments of Donahue *et al.* (2010*b*) with silicon oils and steel balls, reported parameters are: $\nu = 0.35$, $E = 1.93 \times 10^{11}$ Pa, $a = 0.00635$ m, $\mu = 12$ Pa s, $p_{gt} = 500$ MPa and $v_r = 0.5$ m s^{-1}. Under these conditions, $h_e \approx 5$ μm and $h_g \approx 18$ μm, both larger than the roughness size of $h_b \approx 1$ μm. Note that, when h_e or h_g dominates as in this case, increasing St by increasing v_r (with all else constant) also increases h_{min}, which strengthens the rebound. Thus, Donahue *et al.* (2010*b*)

used the glass-transition criterion and saw (by both simulation and experiment) a faster increase in the wet coefficient of restitution with increasing Stokes number than predicted for h_{min} fixed.

A very different situation occurs for low-viscosity liquids. In the experiments of Buck *et al.* (2018) with glass beads and water, for example, typical parameters are $E = 7 \times 10^9$ Pa, $\nu = 0.2$, $\mu = 1$ mPa s, $a = 0.001$ m, $v_r = 1$ m s^{-1} and $p_{gt} = 900$ MPa (at 20 °C). Then, $h_e = 0.2$ μm and $h_g = 0.06$ μm are both smaller than the average surface roughness of a few microns. Thus, a constant value of h_{min} (and, hence, St_s) may be employed.

6.4. *Comparison with experiments*

As noted previously, experiments on collisions of three wet spheres were reported by Donahue *et al.* (2010*a*,*b*). They used a pendulum setup to achieve Stokes numbers in the desired range and to keep the collisions rectilinear (as long as the departures of the pendulum strings from vertical were small, so that long strings were used). As a first test of the model, and to find the glass-transition pressure, figure 16 shows the wet coefficient of restitution for the collision of two stainless-steel spheres ($e_{dry} = 0.90$, $E = 1.93 \times 10^{11}$ Pa, $\nu = 0.35$, $a = 0.00635$ m, $m = 0.0336$ kg) or two chrome-steel spheres ($e_{dry} = 0.99$, $E = 2.03 \times 10^{11}$ Pa, $\nu = 0.28$, $a = 0.00635$ m, $m = 0.0328$ kg). The stainless-steel spheres had combined oil layers of thickness $h_{12}^0 = 294$ μm and viscosity 12 Pa s. The chrome-steel spheres had a combined oil-layer thickness of 180 μm and viscosity of 5.1 Pa s. The symbols are the experimental data from figure 7 of Donahue *et al.* (2010*b*). The solid lines are the analytical theory from the current work (equations (5.5), (5.7) and (5.11)) with $h_{min} = h_g$ given by (6.4) and thus varying with impact velocity, and the dashed lines are the analytical theory with h_{min} fixed at its value for $St = St_s$. Following Donahue *et al.* (2012*a*), the value of $p_{gt} = 21$ MPa was selected so that $St_s = 1.7$ matches the experimental results for when rebound of the chrome-steel spheres was first observed. For the stainless-steel spheres and more viscous oil, the corresponding fit is $St_s = 1.5$ and $p_{gt} = 26$ Mpa. Note that these values are lower than typical glass-transition pressures of 300–700 MPa at room temperature reported for other lubricating and silicon oils (Angel *et al.* 2007; Bair 2019). However, since the viscosity of a fluid increases very rapidly with pressure within 1–2 orders of magnitude of its glass transition (Bair 2019), it is anticipated that high lubrication forces would arrest the relative motion before the full glass transition is reached. Moreover, these pressures are lower than the yield strength (∼300–400 MPa) of the steel spheres, and so plastic deformation was not anticipated (nor observed). As expected, the agreement between theory and experiment in figure 16 is better when h_{min} varies according to (6.4) than when it is fixed. The rate of increase in the wet coefficient of restitution with Stokes number is higher for the chrome-steel spheres, due to their higher value of e_{dry}.

In the three-sphere experiments of Donahue *et al.* (2010*a*,*b*), the liquid layers on the target and far-side spheres were initially in contact, so that $d_{23}^0 = 0$ and simultaneous collisions were the norm. The coating process gave an excess of fluid in the vicinity of contact for the 2–3 pair, so $h_{23}^f > h_{12}^0$. Also, due to capillary forces that drew the 2–3 pair together prior to the collision, $h_{23}^0 \ll h_{12}^0$. The very small initial separation of the 2–3 pair meant that this pair was essentially in solid–solid contact before the collision, either on roughness elements or more likely such that a glass transition would prevent any significant relative motion toward one another. To model this situation, the 2–3 pair was treated as a doublet without relative motion, until the striker sphere 1 made

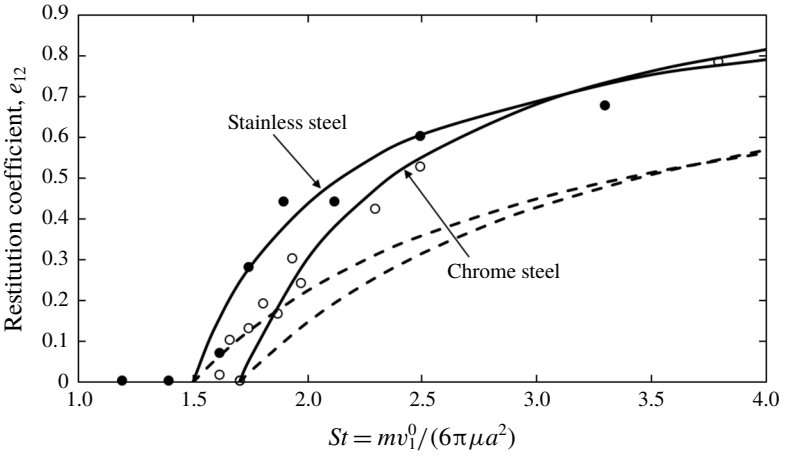

FIGURE 16. Wet coefficient of restitution versus Stokes number for the head-on collision of two stainless-steel (●) or chrome-steel (○) balls coated with a viscous oil. The experimental data are from Donahue *et al.* (2010*b*), the solid lines are the current theory with $h_{min} = h_g$ from (6.4) and the dashed lines are the theory with h_{min} fixed.

contact with the target sphere 2, at which point its momentum was transferred to sphere 3 and the 2–3 pair began to separate. The simulation of the first stage of approach is still governed by (4.1) in this situation, except that $\hat{v}_{23} = 0$ and the Stokes number is replaced by 4/3 of the original value, to account for the combined mass of the 2–3 doublet. The post-contact velocities of (4.3) are replaced by

$$v_{12}^a = [(1 + e_{dry})^2/4 - e_{dry}]v_{12}^b, \quad v_{23}^a = -e_{dry}(1 + e_{dry})v_{12}^b/2 \tag{6.5a,b}$$

as momentum is transferred from sphere 1 to sphere 2 and then sphere 2 to sphere 3 in a double collision. The subsequent relative motion of both pairs was then analysed using (4.1) without modification. Figure 17 provides an example comparison between the present experiments and the current theory for the chrome-steel spheres and the oil of viscosity 12 Pa. The combined film thicknesses are $h_{12}^0 = 412$ μm and $h_{23}^f = 1534$ μm, with a nominal initial separation of the 2–3 pair of $h_{23}^0 = 10$ μm (but with a measurement uncertainty of 10 μm). The glass-transition pressure used in the model is $p_{gt} = 26$ MPa, as determined from the two-sphere results for the more viscous oil. From (6.4), the glass transition and, hence, collision and rebound of the *i*–*j* pair occur when

$$h_{ij} \leqslant (3\mu a v_{ij}/p_{gt})^{1/2}. \tag{6.6}$$

This equation may be rearranged and non-dimensionalized as

$$\hat{v}_{ij}/\hat{h}_{ij}^2 \geqslant Pg = Pg_{ref}/St, \tag{6.7}$$

where $Pg = p_{gt}(h_{12}^0)^2/(3\mu a v_1^0)$ is a dimensionless glass-transition pressure. For comparison to a set of experiments in which v_1^0 (and, hence, St) is varied, but all other physical parameters are fixed, it is convenient to define $Pg_{ref} = p_{gt}(h_{12}^0)^2/(3\mu a v_{ref}) = mp_{gt}(h_{12}^0)^2/(18\pi\mu^2 a^3)$ as a reference pressure and $v_{ref} = 6\pi\mu a^2/m$ as a reference velocity that yields $St = 1$. In the experiments of Donahue *et al.* (2010*a*,*b*), $Pg_{ref} = O(10^2)$, indicating

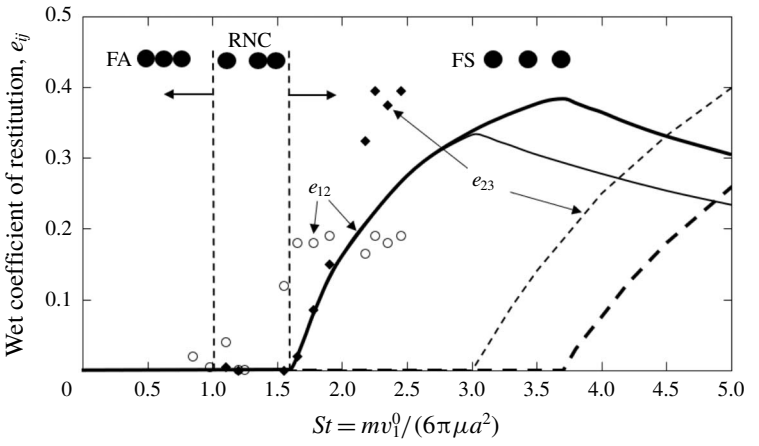

FIGURE 17. Wet coefficients of restitution versus Stokes number for the head-on collision of three chrome-steel spheres covered with oil layers of viscosity 12 Pa s and thicknesses $h_{12}^0 = 412$ μm and $h_{23}^f = 1534$ μm. The nominal initial separation of the 2–3 pair is $h_{23}^0 = 10$ μm, but it may vary in the range 1–20 μm. The symbols are experiments from Donahue *et al.* (2010*b*) and the curves are the current theory with $h_{23}^0 = 10$ μm (thick lines) and 20 μm (thin lines).

that substantial penetration into the liquid layer ($\hat{h}_{ij} \ll 1$) is required for the rebound criterion to be met. Note that Pg_{ref} is independent of particle size but has strong dependence on the liquid-layer thickness and viscosity.

As seen in figure 17, there is qualitative agreement between theory and experiment when $h_{23}^0 = 10$ μm is used as the initial separation for the 2–3 doublet. According to the theory, full agglomeration with $e_{12} = e_{23} = 0$ occurs for $St < 1.6$, reverse Newton's cradle with e_{12} increasing and $e_{23} = 0$ occurs for $1.6 < St < 3.8$, and full separation (FS) with e_{12} nearly flat and e_{23} increasing occurs for $St > 3.8$. The experimental data show the same behaviour, except the boundaries between the different outcomes are shifted to lower Stokes numbers. This difference could be due to cavitation or another factor reducing the viscous resistance to rebound or to the uncertainty in the very small initial gap between the 2–3 pair. Donahue *et al.* (2010*b*) noted that the uncertainty in measuring the initial gap and oil-layer thickness is approximately 10 μm, so that the actual value of the initial 2–3 gap could be in the range 1 μm $< h_{23}^0 <$ 20 μm (where the lower limit is an estimated minimum roughness height). Rerunning the simulations for $h_{23}^0 = 20$ μm gives qualitatively similar results as for $h_{23}^0 = 10$ μm, but the separation of the 2–3 pair is stronger and that of the 1–2 pair is weaker, with somewhat better agreement with experiments.

Figure 18 provides a further comparison of the current model with experimental data. For this figure, the oil had lower viscosity ($\mu = 5.1$ Pa s) and thinner layers ($h_{12}^0 = 280$ μm and $h_{23}^f = 1106$ μm). The nominal initial separation between the 2–3 pair is again $h_{23}^0 = 10$ μm. Simulations with this value again yield qualitative agreement with the experiments. However, simulations with $h_{23}^0 = 20$ μm, which is at the upper range of measurement uncertainty, show relatively good agreement with the experiments. The agreement between the present model and the experiments is better than found in the prior work of Donahue *et al.* (2010*b*). One reason for the improved agreement is that the present work treats the glass-transition pressure as

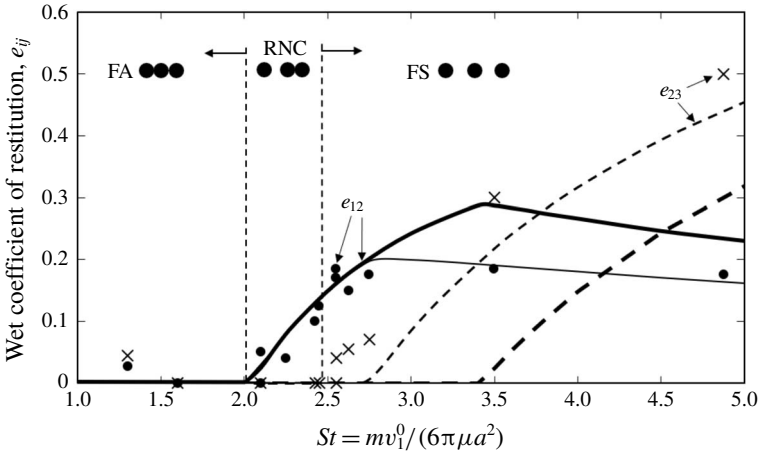

FIGURE 18. Wet coefficients of restitution versus Stokes number for the head-on collision of three chrome-steel spheres covered with oil layers of viscosity 5.1 Pa s and thicknesses $h_{12}^0 = 280$ μm and $h_{23}^f = 1106$ μm. The nominal initial separation of the 2–3 pair is $h_{23}^0 = 10$ μm, but it may vary in the range 1–20 μm. The symbols are experiments from Donahue *et al.* (2010*b*) and the curves are the current theory with $h_{23}^0 = 10$ μm (thick lines) and 20 μm (thin lines).

a fitting parameter found from the two-sphere experiments. Another reason is the simultaneous treatment of the three-sphere interaction in the present work, rather than modelling it as a series of two-body interactions. In particular, after sphere 1 hits the 2–3 doublet, sphere 3 begins to move away from sphere 2. The lubrication suction force then pulls sphere 2 away from sphere 1, which in turn creates a lubrication suction force between the 1–2 pair. The ultimate outcome (FA, NC, RNC or FS) depends on a sensitive interplay of these simultaneous forces.

Finally, the underlying assumption that the collisions may be treated as soft-sphere collisions during the approach and rebound through the intervening liquid layers, and as hard-sphere collisions when contact and velocity reversal occur, was checked. From Hertzian impact theory for the collision of two solid spheres, the solid–solid contact time scales as $t_h = O[(\rho_s^2\theta^2/v_r)^{1/5}a]$ (Davis *et al.* 1986), where ρ_s is the solid density. For the experiments of Donahue *et al.* (2010*b*), this hard-sphere contact time scale is $t_h \approx 10^{-5}$ s. In contrast, the soft-sphere collision time scale is $t_s = O(v_r/h_0) \approx 10^{-3}$ s. Since $t_h \ll t_s$, the approximation of the contact/reversal stage as an instantaneous, hard-sphere collision is justified. For collisions with softer materials such as glass (Buck *et al.* 2018), this condition is still met, but the difference is only one order of magnitude.

7. Concluding remarks

The rectilinear collision of three spheres covered with thin liquid layers has been investigated by analytical (sequential doublet collisions) and numerical (simultaneous triplet collisions) methods. As originally demonstrated by Donahue *et al.* (2010*a*,*b*), four primary outcomes are observed: full agglomeration of all three spheres, full separation of the three spheres, Newton's cradle where the striker and target sphere stick together but the third (far-side) sphere separates and reverse Newton's cradle

where the target and far-side sphere stick together while the striker sphere rebounds away. When there is an initial air gap between the target and far-side sphere, which is expected to be important in practice but not previously studied, more exotic behaviour is observed, such as FS/FA or FS/NC, where the three spheres fully separate after the initial collision(s) but then undergo subsequent collisions that result in full or partial agglomeration.

The results are presented in dimensionless form, with several governing parameters. As with prior studies on wet two-sphere or sphere-surface collisions, the most important parameter is the Stokes number, representing the ratio of inertia and viscous forces. In physical terms, the Stokes number increases with increasing sphere density, radius and impact velocity, and decreases with increasing fluid viscosity. For Stokes numbers below a critical value, full agglomeration is observed, whereas large Stokes numbers yield full separation and/or Newton's cradle. Reverse Newton's cradle is predicted for intermediate Stokes numbers, but only when there is a thicker combined final liquid layer on the target and far-side spheres than on the striker and target spheres. Reverse Newton's cradle was demonstrated (via simulation and experiment) by Donahue *et al.* (2010*a*,*b*) and results from the thicker liquid layer dampening the collision and holding the target–far-side pair together.

Another parameter in the analysis is the dry coefficient of restitution, as a hard-sphere reversal of the relative velocity and with energy loss described by this coefficient were assumed when contact was made. A decrease in the dry coefficient of restitution increases the critical Stokes number for separation in a simple, predictable manner. The dry coefficient of restitution was treated as a constant in the present work, but a relatively simple change would be to allow it to vary with impact speed.

Yet another key parameter is the minimum separation of the nominal sphere surfaces at which contact and velocity reversal are assumed to occur. When this value made dimensionless with the liquid film thickness is small, the critical Stokes number for rebound and separation is proportional to its natural logarithm. Thus, smaller values of the minimum separation yield larger critical Stokes numbers, because there are greater viscous losses as the colliding surfaces penetrate further into the liquid film. Following prior work, three mechanisms are presented for the minimum separation: a bump or roughness height, an elastohydrodynamic deformation length, and a glass-transition separation distance, with the dominate mechanism based on the largest of these values. For low-viscosity liquids, or rough surfaces, the roughness height is expected to dominate. Then, the dimensionless minimum separation is easily varied in practice, independently of the Stokes number, simply by varying the liquid film thickness. For high-viscosity liquids and smooth surfaces, the glass-transition or elastohydrodynamic minimum separation is expected to dominate. Then, both the minimum separation and the Stokes number depend on physical quantities such as the sphere radius, relative velocity and fluid viscosity. The present analysis still holds, but the dimensionless minimum separation at which rebound is initiated as part of the relative-velocity versus separation-gap solution and depends on a dimensionless glass-transition or elasticity parameter. This finding leads to the question of whether or not glass-transition and/or elastohydrodynamic deformation needs to be considered in simulations of flows of particles or grains fully immersed in a fluid. The key to addressing this issue is to estimate the maximum lubrication pressure and compare it to the glass-transition pressure of the liquid and the Young's modulus of the solid. For example, if $\mu = 0.1$ Pa s (100 times the viscosity of water), $a = 10^{-2}$ m, $v_r = 1$ m s^{-1} and $h = 3$ μm, then the dynamic lubrication pressure is $p_d = 3\mu a v_r/h^2 \approx 300$ MPa, which is comparable to typical glass-transition pressures but small compared to

Young's moduli of hard materials. For collisions in less viscous fluids or with small relative velocities, these effects are likely negligible.

Finally, the current analysis points the way for a variety of future studies. One is the inclusion of capillary forces in collisions of wetted spheres when the modified capillary number is of order unity, and also for larger capillary numbers but near the critical conditions for rebound and separation. Another is to examine the effects of rotation and sliding lubrication forces (along with frictional contact forces) for oblique collisions of multiple wetted spheres. Then, once these collision mechanisms and models are sufficiently understood, they may be incorporated in discrete-element models to improve the simulations of wet granular flows involving many wet particles (e.g. Anand *et al.* 2009; Kantak, Hrenya & Davis 2009; Radl *et al.* 2010; Liu *et al.* 2013).

Acknowledgements

R.H.D. initiated this work while visiting the University of Canterbury as an Erskine Fellow; he thanks D. Holland for conversations about the model. He also thanks S. Baysinger for help with the manuscript and figures.

REFERENCES

ANAND, A., CURTIS, J. S., WASSGREN, C. R., HANCOCK, B. C. & KETTERHAGEN, W. R. 2009 Predicting discharge dynamics of wet cohesive particles from a rectangular hopper using the discrete element method (DEM). *Chem. Engng Sci.* **64**, 5268–5275.

ANGEL, R. J., BUJAK, M., ZHAO, J., GATTA, G. D. & JACOBSEN, S. D. 2007 Effective hydrostatic limits of pressure media for high-pressure crystallographic studies. *J. Appl. Crystallogr.* **40**, 26–32.

BAIR, S. 2019 The viscosity at the glass transition of a liquid lubricant. *Friction* **7**, 86–91.

BARNOCKY, G. & DAVIS, R. H. 1988 Elastohydrodynamic collision and rebound of spheres: experimental verification. *Phys. Fluids* **31**, 1324–1329.

BARNOCKY, G. & DAVIS, R. H. 1989 The influence of pressure-dependent density and viscosity on the elastohydrodynamic collision and rebound of two spheres. *J. Fluid Mech.* **209**, 501–519.

BORDBAR, M. H. & HYPPÄNEN, T. 2007 Modeling of binary collisions between multisize viscoelastic spheres. *J. Numer. Anal. Ind. Appl. Maths* **2**, 115–118.

BRAKE, M. R. W., REU, P. L. & ARAGON, D. S. 2017 A comprehensive set of impact data for common aerospace metals. *J. Comput. Nonlinear Dyn.* **12**, 061011.

BUCK, B., LUNEWSKI, J., TANG, Y., DEEN, N. G., KUIPERS, J. A. M. & HEINRICH, S. 2018 Numerical investigation of collision dynamics of wet particles via force balance. *Chem. Engng Res. Des.* **132**, 1143–1159.

BUCK, B., TANG, Y., HEINRICH, S., DEEN, N. G. & KUIPERS, J. A. M. 2017 Collision dynamics of wet solids: rebound and rotation. *Powder Technol.* **316**, 218–224.

CRUGER, B., SALIKOV, V., HEINRICH, S., ANTONYUK, S., SUTKAR, V., DEEN, N. & KUIPERS, J. A. M. 2016 Coefficient of restitution for particles impacting on wet surfaces: an improved experimental approach. *Particuology* **25**, 1–9.

DAVIS, R. H., RAGER, D. A. & GOOD, B. T. 2002 Elastohydrodynamic rebound of spheres from coated surfaces. *J. Fluid Mech.* **468**, 107–119.

DAVIS, R. H., SERAYSSOL, J. M. & HINCH, E. J. 1986 The elastohydrodynamic collision of two spheres. *J. Fluid Mech.* **163**, 479–497.

DONAHUE, C. M., BREWER, W. M., DAVIS, R. H. & HRENYA, C. M. 2012*a* Agglomeration and de-agglomeration of rotating wet doublets. *J. Fluid Mech.* **708**, 128–148.

DONAHUE, C. M., DAVIS, R. H., KANTAK, A. A. & HRENYA, C. M. 2012*b* Mechanisms for agglomeration and de-agglomeration following oblique collisions of wet particles. *Phys. Rev.* E **86**, 021303.

DONAHUE, C. M., HRENYA, C. M. & DAVIS, R. H. 2010*a* Stokes' cradle: Newton's cradle with liquid coating. *Phys. Rev. Lett.* **105**, 034501.

DONAHUE, C. M., HRENYA, C. M., DAVIS, R. H., NAKAGAWA, K. J., ZELINSKAYA, A. P. & JOSEPH, G. G. 2010*b* Stokes' cradle: normal three-body collisions between wetted particles. *J. Fluids Mech.* **650**, 479–504.

JOSEPH, G. G. & HUNT, M. L. 2004 Oblique particle–wall collisions in a liquid. *J. Fluid Mech.* **510**, 71–93.

JOSEPH, G. G., ZENIT, R., HUNT, M. L. & ROSENWINKEL, A. M. 2001 Particle–wall collisions in a viscous fluid. *J. Fluid Mech.* **433**, 329–346.

KANTAK, A. A. & DAVIS, R. H. 2004 Oblique collisions and rebound of spheres from a wetted surface. *J. Fluid Mech.* **509**, 63–81.

KANTAK, A. A. & DAVIS, R. H. 2006 Elastohydrodynamic theory for wet oblique collisions. *Powder Technol.* **168**, 42–52.

KANTAK, A. A., HRENYA, C. M. & DAVIS, R. H. 2009 Initial rates of aggregation for dilute, granular flows of wet (cohesive) particles. *Phys. Fluids* **21**, 023301.

LIAN, G., ADAMS, M. J. & THORNTON, C. 1996 Elastohydrodynamic collisions of solid spheres. *J. Fluid Mech.* **311**, 141–152.

LIU, P. Y., YANG, R. Y. & YU, A. B. 2013 The effect of liquids on radial segregation of granular mixtures in rotating drums. *Granul. Matt.* **15**, 427–436.

MA, J., LIU, D. & CHEN, X. 2016 Normal and oblique impacts between smooth spheres and liquid layers: liquid bridge and restitution coefficient. *Power Technol.* **301**, 747–759.

MARSTON, J. O., YONG, W., NG, W. K., TAN, R. B. H. & THORODDSEN, S. T. 2011 Cavitation structures formed during the rebound of a sphere from a wetted surface. *Exp. Fluids* **50**, 729–746.

MIKAMI, T., KAMIYA, H. & HORIO, M. 1998 Numerical simulation of cohesive powder behavior in a fluidized bed. *Chem. Engng Sci.* **53**, 1927–1940.

RADL, S., KALYODA, E., GLASSER, B. J. & KHINAST, J. G. 2010 Mixing characteristics of wet granular matter in a bladed mixer. *Powder Technol.* **200**, 171–189.

WEBER, M. W. & HRENYA, C. M. 2006 Square-well model for cohesion in fluidized beds. *Chem. Engng Sci.* **61**, 4511–4527.

XU, Q., ORPE, A. V. & KUDROLLI, A. 2007 Lubrication effects on the flow of wet granular materials. *Phys. Rev.* E **76**, 031302.

YANG, F. L. & HUNT, M. L. 2006 Dynamics of particle–particle collisions in a viscous liquid. *Phys. Fluids* **18**, 121506.